

Beamforming Design for Beyond Diagonal RIS-Aided Cell-Free Massive MIMO Systems

Yizhuo Li, Jiakang Zheng, *Member, IEEE*, Bokai Xu, Yiyang Zhu,
Jiayi Zhang, *Senior Member, IEEE*, Dusit Niyato, *Fellow, IEEE* and Bo Ai, *Fellow, IEEE*

Abstract—Reconfigurable intelligent surface (RIS)-aided cell-free (CF) massive multiple-input multiple-output (mMIMO) is a promising technology for further improving spectral efficiency (SE) with low cost and power consumption. However, conventional RIS has inevitable limitations due to its diagonal scattering matrix. In contrast, beyond-diagonal RIS (BD-RIS) has gained great attention. This correspondence focuses on integrating a hybrid transmitting and reflecting BD-RIS into CF mMIMO systems to enhance coverage and spatial multiplexing. This requires completing the beamforming design under the transmit power constraints and unitary constraints of the BD-RIS, by optimizing active and passive beamformer simultaneously. To tackle this issue, we introduce an alternating optimization algorithm that decomposes it using fractional programming and solves the subproblems alternatively. Moreover, to address the challenge introduced by the unitary constraint on the beamforming matrix of the BD-RIS, we propose a Riemannian limited-memory Broyden-Fletcher-Goldfarb-Shanno (R-L-BFGS) algorithm to solve the problem optimally. Simulation results show that our algorithm achieves faster convergence and finds higher-quality solutions compared with baselines, while also demonstrating a favorable performance-complexity trade-off.

Index Terms—Beyond-diagonal RIS, cell-free massive MIMO, spectral efficiency, beamforming design.

I. INTRODUCTION

The upcoming sixth generation (6G) network is anticipated to play a key role in many areas of society, industry and daily life in the future, requiring extremely high communication standards in terms of capacity, latency, reliability and intelligence [1], [2]. In the future, cell-free (CF) massive multiple-input multiple-output (mMIMO) systems are expected to replace traditional cellular systems in empowering the upcoming 6G [3]–[6]. By distributing access points (APs) across a wide area and connecting them to a central processing unit (CPU), CF mMIMO systems can offer high data rates, low latency, and efficient resource utilization. Moreover, reconfigurable

intelligent surfaces (RISs) have deployed as an economical solution in the CF mMIMO system [7]–[9].

RIS is an advanced technology that enhances signal propagation and quality by using a large array of passive, low-cost reflective elements to dynamically adjust the phase and amplitude of incident electromagnetic waves. However, traditional RIS inevitably has limitations in complex scenarios because the scattering matrix must be diagonal. To address the limitations of RIS, the beyond-diagonal RIS (BD-RIS) has been proposed as a novel evolution [10]. Unlike traditional RIS, BD-RIS exhibits a non-diagonal scattering matrix. Depending on the interconnection schemes among the elements, BD-RIS can be classified into: single-connected (SC), fully-connected (FC), group-connected (GC), tree-connected, band-connected [11] and stem-connected [12] architectures. According to the arrangement of elements for each architecture, BD-RIS has three modes: reflecting mode, hybrid transmitting and reflecting mode and multi-sector mode [10].

The recent researchs have delved into BD-RIS-aided systems. The performance of BD-RISs with different modes/architectures in multiuser multiple input single output (MU-MISO) system had been studied comprehensively in [10]. The authors in [13] conducted an in-depth study of the performance of STAR-RIS in CF mMIMO systems. Although STAR-RIS introduced the concept of hybrid transmission and reflection, it is fundamentally a single-connected (SC) architecture. This authors in [14] evaluates the performance of a BD-RIS-aided CF mMIMO for simultaneous wireless information and power transfer (SWIPT) under practical channel and energy harvesting assumptions. And the authors of [15] consider a BD-RIS-aided multi-user system and use iterative closed-form solutions to alternately optimize active and passive beamforming matrices. The aforementioned works have showcased the outstanding performance of BD-RIS in communication systems. However, to the best of our knowledge, the performance of hybrid BD-RIS in more architecture in CF mMIMO systems has not been studied.

In this correspondence, we investigate the integration of a hybrid transmitting and reflecting BD-RIS into CF mMIMO systems to enhance both coverage and spatial multiplexing. The main contributions are summarized as follows:

- We develop a unified beamforming design framework that enables a comprehensive performance comparison among various BD-RIS architectures, including SC, GC, and FC.
- To effectively solve the non-convex optimization problem, we propose a Riemannian limited-memory Broyden-Fletcher-Goldfarb-Shanno (R-L-BFGS) algorithm, which offers a robust and efficient solution.

This work was supported in part by National Natural Science Foundation of China under Grant 62501042, Grant 62471027, Grant 62221001, and Grant 62341127; in part by China Postdoctoral Science Foundation under Grant BX20250378 and Grant 2024M760195; in part by the Talent Fund of Beijing Jiaotong University under Grant 2024XKRC085; in part by Jiangxi Province Science and Technology development Programme under Grant 20242BCC32016; in part by the Fundamental Research Funds for the Central Universities under Grant 2025JBZX037; and in part by ZTE Industry-Institute Cooperation Funds under Grant No. IA20250115003-PO0001. (*Corresponding author: Jiakang Zheng.*)

Y. Li, J. Zheng, B. Xu, J. Zhang, and B. Ai are with State Key Laboratory of Advanced Rail Autonomous Operation, and also with School of Electronic and Information Engineering, Beijing Jiaotong University, Beijing 100044, P. R. China (e-mail: jiakangzheng, jiyizhang, boai@bjtu.edu.cn).

Y. Zhu is with the School of Electrical and Electronics Engineering, Nanyang Technological University, Singapore 639798.

D. Niyato is with the College of Computing and Data Science, Nanyang Technological University, Singapore 639798 (e-mail: dniyato@ntu.edu.sg).

- Simulation results demonstrate that the proposed R-L-BFGS algorithm achieves faster convergence and attains higher-quality solutions compared with baselines.

II. SYSTEM MODEL

We focus on a BD-RIS-aided CF mMIMO system. The system consists of L APs, K UEs, and one BD-RIS. Each AP and UE consist of N antennas and one antenna, respectively. The BD-RIS has M cells, each consisting of two back-to-back antennas interconnected via reconfigurable admittance components [10]. The BD-RIS serves K_r reflective and K_t transmissive UEs, with a total of $K = K_r + K_t$. Let $\mathcal{L} = \{1, \dots, L\}$, $\mathcal{K}_r = \{1, \dots, K_r\}$, $\mathcal{K}_t = \{1, \dots, K_t\}$ and $\mathcal{K} = \{1, \dots, K\}$ represent the index sets for APs, reflective UEs, transmissive UEs and all UEs respectively. We assume perfect channel state information (CSI) is available at the APs. Then, the channel from the l -th AP to the k -th UE is

$$\mathbf{h}_{l,k}^H = \mathbf{f}_k^H \Theta_i \mathbf{G}_l + \mathbf{h}_{l,k,d}^H, \forall i \in \{t, r\}, \forall k \in \mathcal{K}_i, \quad (1)$$

where $\mathbf{f}_k \in \mathbb{C}^M$, $\mathbf{h}_{l,k,d} \in \mathbb{C}^N$ and $\mathbf{G}_l \in \mathbb{C}^{M \times N}$ represent the frequency-domain channel from the BD-RIS to the UE k , from the AP l to the UE k and from the AP l to the BD-RIS, respectively. In the GC BD-RIS, the M cells are partitioned into G groups, denoted by $\mathcal{G} = \{1, \dots, G\}$. Each group has an equal size $\bar{M} = M/G$. Other BD-RIS scenarios can be handled by adjusting G accordingly. We consider that each group has an equal size, denoted as $\bar{M} = M/G$. In the hybrid BD-RIS, the scattering matrix Θ is divided into Θ_r and Θ_t . Θ_r and Θ_t are block diagonal matrices, expressed as: $\Theta_r = \text{blkdiag}(\Theta_{r,1}, \dots, \Theta_{r,G})$, $\Theta_t = \text{blkdiag}(\Theta_{t,1}, \dots, \Theta_{t,G})$, where $\Theta_{t,g}, \Theta_{r,g} \in \mathbb{C}^{\bar{M} \times \bar{M}}, \forall g \in \mathcal{G}$ satisfy the constraint: $\Theta_{r,g}^H \Theta_{r,g} + \Theta_{t,g}^H \Theta_{t,g} = \mathbf{I}_{\bar{M}}$. Thus the received signal by the k -th UE is

$$y_k = \mathbf{h}_k^H \mathbf{w}_k s_k + \sum_{j=1, j \neq k}^K \mathbf{h}_k^H \mathbf{w}_j s_j + n_k, \quad (2)$$

where $n_k \sim \mathcal{CN}(0, \sigma_k^2)$ denotes the additive white Gaussian noise, $s_k, \forall k \in \mathcal{K}$ denotes the transmitted symbol to the k -th UE, $\mathbf{w}_{l,k} \in \mathbb{C}^N$ is the active beamformer for UE k at the l -th AP. And we defined $\mathbf{h}_k = [\mathbf{h}_{1,k}^T, \dots, \mathbf{h}_{L,k}^T]^T \in \mathbb{C}^{LN}$ and $\mathbf{w}_k = [\mathbf{w}_{1,k}^T, \dots, \mathbf{w}_{L,k}^T]^T \in \mathbb{C}^{LN}$. Then, the signal-to-interference-plus-noise ratio for each UE is derived as

$$\gamma_k = |\mathbf{h}_k^H \mathbf{w}_k|^2 / \left(\sum_{j \in \mathcal{K}, j \neq k} |\mathbf{h}_k^H \mathbf{w}_j|^2 + \sigma_k^2 \right), \forall k \in \mathcal{K}. \quad (3)$$

Moreover, the SE maximization problem is formulated as

$$\mathcal{P}^0 : \max_{\mathbf{w}, \Theta_t, \Theta_r} \text{sum-SE} = \sum_{k \in \mathcal{K}} \log_2(1 + \gamma_k) \quad (4a)$$

$$\text{s.t. } C_1 : \Theta_{r,g}^H \Theta_{r,g} + \Theta_{t,g}^H \Theta_{t,g} = \mathbf{I}_{\bar{M}}, \forall g \in \mathcal{G}, \quad (4b)$$

$$C_2 : \sum_{k=1}^K \|\mathbf{w}_{l,k}\|^2 \leq P_{l,\max}, \quad (4c)$$

where $P_{l,\max}$ is the maximum transmit power of the l -th AP and $\mathbf{w} = [\mathbf{w}_1^T, \dots, \mathbf{w}_K^T]^T \in \mathbb{C}^{KLN}$ is defined for simplicity.

III. BEAMFORMING DESIGN

A. Overview of the Beamforming Design Framework

Utilizing the Lagrangian dual transform and quadratic transform [16], the objective sum-SE can be restated as follows:

$$f_\tau(\mathbf{w}, \Theta_t, \Theta_r, \rho, \tau) = \sum_{k \in \mathcal{K}} \left(\log_2(1 + \rho_k) - \rho_k + 2\sqrt{1 + \rho_k} \Re\{\tau_k^* \mathbf{h}_k^H \mathbf{w}_k\} - |\tau_k|^2 \sum_{j \in \mathcal{K}} (|\mathbf{h}_k^H \mathbf{w}_j|^2 + \sigma_k^2) \right), \quad (5)$$

where $\rho \triangleq [\rho_1, \dots, \rho_K]^T \in \mathbb{R}^K$, $\tau \triangleq [\tau_1, \dots, \tau_K]^T \in \mathbb{C}^K$. Given fixed $(\mathbf{w}, \Theta_t, \Theta_r, \rho)$ or τ , the optimal τ or ρ can be obtained by solving $\frac{\partial f_\tau}{\partial \tau_k} = 0$ or $\frac{\partial f_\tau}{\partial \rho_k} = 0$ for $\forall k \in \mathcal{K}$. The solution can be written as

$$\rho_k^* = \gamma_k, \tau_k^* = \frac{\sqrt{1 + \rho_k} \mathbf{h}_k^H \mathbf{w}_k}{\sum_{j \in \mathcal{K}} |\mathbf{h}_k^H \mathbf{w}_j|^2 + \sigma_k^2}, \forall k \in \mathcal{K}. \quad (6)$$

B. Active Beamforming: Solve \mathbf{w}

Given $(\Theta_t^*, \Theta_r^*, \rho^*, \tau^*)$, We first define $\mathbf{a} = \sum_{k \in \mathcal{K}} \mathbf{h}_k \tau_k \tau_k^* \mathbf{h}_k^H$, $\mathbf{A} = \mathbf{I}_K \otimes \mathbf{a}$, $\mathbf{v}_k = \mathbf{h}_k \tau_k$. Then, we can extract the equations in (5) associated with \mathbf{w} as

$$g_1(\mathbf{w}) = -\mathbf{w}^H \mathbf{A} \mathbf{w} + \Re\{2\mathbf{v}^H \mathbf{w}\} - Y, \quad (7)$$

where $Y = \sum_{k \in \mathcal{K}} \tau_k^H \sigma_k \tau_k$, $\mathbf{v} = [\mathbf{v}_1^T, \mathbf{v}_2^T, \dots, \mathbf{v}_K^T]^T$. Therefore, the problem can be further simplified as

$$\hat{\mathcal{P}} : \min_{\mathbf{w}} g_2(\mathbf{w}) = \mathbf{w}^H \mathbf{A} \mathbf{w} - \Re\{2\mathbf{v}^H \mathbf{w}\} \quad (8)$$

s.t. $\mathbf{w}^H \mathbf{D}_l \mathbf{w} \leq P_{l,\max}, \forall l \in \mathcal{L}$,

where $\mathbf{D}_l = \mathbf{I}_K \otimes \{(\mathbf{e}_l \mathbf{e}_l^H) \otimes \mathbf{I}_M\}$ with $\mathbf{e}_l \in \mathbb{R}^L$. Since \mathbf{A} and \mathbf{D}_l ($\forall l \in \mathcal{L}$) are all positive semidefinite, the simplified subproblem $\hat{\mathcal{P}}$ is a standard quadratically constrained quadratic program problem. To reduce the complexity, we exploit the *primal-dual subgradient (PDS)* method in [3] to obtain \mathbf{w}^* .

C. Passive Beamforming: Solve $\{\Theta_t, \Theta_r\}$

When \mathbf{w} , ρ and τ are fixed, we can first define

$$\eta_k = \sqrt{1 + \rho_k \tau_k}, \mathbf{g}_k = \sum_{l=1}^L \mathbf{G}_l \mathbf{w}_{l,k}, \quad (9)$$

$$a_{k,j} = \sum_{l=1}^L \mathbf{h}_{l,k,d}^H \mathbf{w}_{l,j}, \forall k \in \mathcal{K}, \forall j \in \mathcal{K},$$

and then the sub-objective function with respect to passive beamformer Θ_t and Θ_r can be written as

$$\sum_{i \in \{t,r\}} \sum_{k \in \mathcal{K}_i} (2\Re\{\mathbf{f}_k^H \Theta_i \mathbf{t}_k\} - |\tau_k|^2 \sum_{j \in \mathcal{K}} |\mathbf{f}_k^H \Theta_i \mathbf{g}_j|^2), \quad (10)$$

where $\mathbf{b}_k \triangleq |\tau_k|^2 \sum_{j \in \mathcal{K}} a_{k,j}^* \mathbf{g}_j$, $\mathbf{t}_k = \eta_k^* \mathbf{g}_k - \mathbf{b}_k, \forall k \in \mathcal{K}$. And (10) can be further reformulated as

$$\sum_{i \in \{t,r\}} \left(2\Re\{\text{Tr}(\Theta_i \mathbf{A}_i)\} - \text{Tr}(\Theta_i \mathbf{B} \Theta_i^H \mathbf{C}_i) \right), \quad (11)$$

where $\mathbf{A}_i \triangleq \sum_{k \in \mathcal{K}_i} \mathbf{t}_k \mathbf{f}_k^H \in \mathbb{C}^{M \times M}$, $\mathbf{B} \triangleq \sum_{j \in \mathcal{K}} \mathbf{g}_j \mathbf{g}_j^H \in \mathbb{C}^{M \times M}$, $\mathbf{C}_i \triangleq \sum_{k \in \mathcal{K}_i} |\tau_k|^2 \mathbf{f}_k \mathbf{f}_k^H \in \mathbb{C}^{M \times M}, \forall i \in \{t, r\}$. However, the quadratic terms in (11) lead to interactions among different groups of $\Theta_{t/r,g}$. To address this, we aim to isolate one specific pair $\Theta_{t,g}$ and $\Theta_{r,g}$ for a given group g while keeping the other pairs fixed, focusing on optimizing the

selected pair. For this purpose, we first reformulate objective in (11) on a group-by-group basis as follows:

$$\sum_{i \in \{t,r\}} (2\Re\{\text{Tr}(\Theta_i \mathbf{A}_i)\} - \text{Tr}(\Theta_i \mathbf{B} \Theta_i^H \mathbf{C}_i)) = \sum_{i \in \{t,r\}} (2 \sum_{q=1}^G (2\Re\{\text{Tr}(\Theta_{i,q} \mathbf{A}_{i,q})\} - \text{Tr}(\sum_{p=1}^G \Theta_{i,p} \sum_{q=1}^G \mathbf{B}_{p,q} \Theta_{i,q}^H \mathbf{C}_{i,q,p}))), \quad (12)$$

where

$$\begin{aligned} \mathbf{A}_{i,q} &= [\mathbf{A}_i]_{(q-1)\bar{M}+1:q\bar{M},(q-1)\bar{M}+1:q\bar{M}}, \\ \mathbf{B}_{p,q} &= [\mathbf{B}]_{(p-1)\bar{M}+1:p\bar{M},(q-1)\bar{M}+1:q\bar{M}}, \\ \mathbf{C}_{i,q,p} &= [\mathbf{C}_i]_{(q-1)\bar{M}+1:q\bar{M},(p-1)\bar{M}+1:p\bar{M}}, \forall p, q \in \mathcal{G}. \end{aligned} \quad (13)$$

When focusing on a single pair $\Theta_{t,g}$ and $\Theta_{r,g}$, the resulting sub-objective function takes the following form:

$$\begin{aligned} f_g(\Theta_{t,g}, \Theta_{r,g}) &= \sum_{i \in \{t,r\}} \left(\text{Tr}(\Theta_{i,g} \mathbf{B}_{g,g} \Theta_{i,g}^H \mathbf{C}_{i,g,g}) \right. \\ &\quad \left. - 2\Re\{\text{Tr}(\Theta_{i,g} (\mathbf{A}_{i,g} - \underbrace{\sum_{p \neq g} \mathbf{B}_{g,p} \Theta_{i,p}^H \mathbf{C}_{i,p,g}}_{\mathbf{X}_{i,g}}))\} \right). \end{aligned} \quad (14)$$

Define matrices $\Theta_g \triangleq [\Theta_{t,g}^H, \Theta_{r,g}^H]^H$, $\mathbf{X}_g \triangleq [\mathbf{X}_{t,g}, \mathbf{X}_{r,g}]$, and $\mathbf{C}_g \triangleq \text{blkdiag}(\mathbf{C}_{t,g,g}, \mathbf{C}_{r,g,g})$. We can then express the sub-problem related to Θ_g as follows:

$$\min_{\Theta_g} \tilde{f}_g(\Theta_g) = \text{Tr}(\Theta_g \mathbf{B}_{g,g} \Theta_g^H \mathbf{C}_g - 2\Re\{\Theta_g \mathbf{X}_g\}) \quad (15a)$$

$$\text{s.t. } \Theta_g^H \Theta_g = \mathbf{I}_{\bar{M}}, \forall g \in \mathcal{G}. \quad (15b)$$

To address the non-convex constraint (15b), we introduce manifold algorithm [17]. (15b) defines an Stiefel manifold:

$$\mathcal{M}_g = \{\Theta_g \in \mathbb{C}^{2\bar{M} \times \bar{M}} : \Theta_g^H \Theta_g = \mathbf{I}_{\bar{M}}, \forall g \in \mathcal{G}\}. \quad (16)$$

And the tangent space for \mathcal{M}_g at $\Theta_{g,k}$ is given by

$$T_{\Theta_{g,k}} \mathcal{M}_g = \{\mathbf{T}_g \in \mathbb{C}^{2\bar{M} \times \bar{M}} : \Re\{(\Theta_{g,k})^H \mathbf{T}_g\} = \mathbf{0}_{\bar{M}}\}, \forall g \in \mathcal{G}. \quad (17)$$

The Riemannian gradient can be calculated by projecting the Euclidean gradient onto the tangent space [17]:

$$\text{grad } \tilde{f}_g(\Theta_{g,k}) = \nabla \tilde{f}_g(\Theta_{g,k}) - \Theta_{g,k} \text{chdiag}(\Theta_{g,k})^H \nabla \tilde{f}_g(\Theta_{g,k}), \quad (18)$$

where $\nabla \tilde{f}_g(\Theta_{g,k}) = 2\mathbf{C}_g \Theta_{g,k} \mathbf{B}_{g,g} - 2\mathbf{X}_g^H$, $\forall g \in \mathcal{G}$ and $\text{chdiag}(\cdot)$ chooses all diagonal elements of a matrix to construct a diagonal matrix. The iterative update is given by $\Theta_{g,k+1} = R_{\Theta_{g,k}}(\alpha_k \eta_k)$, where $\Theta_{g,k}$ is the current iterate, $\eta_k \in T_{\Theta_{g,k}} \mathcal{M}_g$ is the search direction in the tangent space, α_k is the step length which can be searched by backtracking algorithms [17], and $R_{\Theta_{g,k}}(\cdot)$ is a retraction mapping a tangent vector back onto the manifold.

1) *Riemannian BFGS Method*: Quasi-Newton methods are highly effective for unconstrained optimization as they build an approximation of the Hessian of the objective function. For simplicity, we define $\mathbf{g}_k = \text{grad } \tilde{f}_g(\Theta_{g,k})$. First, the search direction η_k at iteration k is computed by $\eta_k = -\mathcal{B}_k \mathbf{g}_k$, where \mathcal{B}_k approximates the inverse Hessian matrix and its update is required to satisfy the quasi-Newton condition:

Algorithm 1 R-L-BFGS Two-Loop Recursion

Input: Current gradient \mathbf{g}_k , history buffers $S =$

$$\{\mathbf{s}_i\}_{i=k-m+1}^k, \mathbf{Y} = \{\mathbf{y}_i\}_{i=k-m+1}^k, \mathbf{P} = \{\rho_i\}_{i=k-m+1}^k.$$

Output: New search direction $\eta_{k+1} = -\mathcal{B}_{k+1} \mathbf{g}_{k+1}$.

- 1: $\mathbf{r} = \mathbf{g}_{k+1}$
 - 2: **for** $i = k : k - m + 1$ **do**
 - 3: $\alpha_i = \rho_i \langle \mathbf{s}_i, \mathbf{r} \rangle$
 - 4: $\mathbf{r} = \mathbf{r} - \alpha_i \mathbf{y}_i$
 - 5: **end for**
 - 6: $\mathbf{r} = \mathcal{B}_k^0 \mathbf{r}$
 - 7: **for** $i = k - m + 1 : k$ **do**
 - 8: $\beta = \rho_i \langle \mathbf{y}_i, \mathbf{r} \rangle$
 - 9: $\mathbf{r} = \mathbf{r} + (\alpha_i - \beta) \mathbf{s}_i$
 - 10: **end for**
 - 11: **Return** $\eta_{k+1} = -\mathbf{r}$.
-

$\mathcal{B}_{k+1} \mathbf{s}_k = \mathbf{y}_k$, where $\mathbf{s}_k = \mathcal{T}_{\Theta_{g,k} \rightarrow \Theta_{g,k+1}}(\alpha_k \eta_k)$ and $\mathbf{y}_k = \mathbf{g}_{k+1} - \mathcal{T}_{\Theta_{g,k} \rightarrow \Theta_{g,k+1}}(\mathbf{g}_k)$. We denote the transport of a tangent vector $\eta \in T_{\mathbf{x}} \mathcal{M}$ from the tangent space at point \mathbf{x} to the tangent space at point \mathbf{y} as $\mathcal{T}_{\mathbf{x} \rightarrow \mathbf{y}}(\eta) \in T_{\mathbf{y}} \mathcal{M}$. In the manifold, the update of the variable \mathcal{B}_k is expressed as

$$\mathcal{B}_{k+1} = \left(\mathbf{I} - \frac{\mathbf{s}_k \mathbf{y}_k^T}{\mathbf{s}_k^T \mathbf{y}_k} \right) \tilde{\mathcal{B}}_k \left(\mathbf{I} - \frac{\mathbf{y}_k \mathbf{s}_k^T}{\mathbf{s}_k^T \mathbf{y}_k} \right) + \frac{\mathbf{s}_k \mathbf{s}_k^T}{\mathbf{s}_k^T \mathbf{y}_k} \quad (19)$$

where $\tilde{\mathcal{B}}_k = \mathcal{T}_{\Theta_{g,k} \rightarrow \Theta_{g,k+1}} \circ \mathcal{B}_k \circ \mathcal{T}_{\Theta_{g,k+1} \rightarrow \Theta_{g,k}}^{-1}$ [18]. The above formulas are somewhat different from the established theories of Euclidean geometry. That is because we need to ensure that all vector and operator operations are performed in the same tangent space on the manifold. However, the R-BFGS method requires the storage and updating of an explicit matrix representation of the operator \mathcal{B}_k . This drawback renders the full R-BFGS method impractical.

2) *Proposed Riemannian L-BFGS*: To overcome the high complexity of the R-BFGS method, we propose a R-L-BFGS algorithm. The key idea of L-BFGS is to avoid forming, storing, and updating the dense inverse Hessian approximation \mathcal{B}_k . Instead, it only stores a limited history of the m most recent displacement and gradient-difference vector pairs, $\{(\mathbf{s}_i, \mathbf{y}_i)\}_{i=k-\hat{m}}^k$, where $\hat{m} = \min\{k, m-1\}$. Based on the full BFGS update formula similar to (19), the iterative formula for the L-BFGS method can be derived as:

$$\begin{aligned} \mathcal{B}_{k+1} &= (\mathbf{V}_k^T \mathbf{V}_{k-m+1}^T) \mathcal{B}_k^0 (\mathbf{V}_{k-m+1} \mathbf{V}_k) + \rho_{k-m+1} \\ &\quad \times (\mathbf{V}_k^T \mathbf{V}_{k-m+2}^T) \mathbf{s}_{k-m+1} \mathbf{s}_{k-m+1}^T (\mathbf{V}_{k-m+2} \mathbf{V}_k) \\ &\quad + \dots + \rho_k \mathbf{s}_k \mathbf{s}_k^T, \end{aligned} \quad (20)$$

where $\rho_i = 1/\langle \mathbf{s}_i, \mathbf{y}_i \rangle$, $\mathbf{V}_i = (\mathbf{I} - \rho_i \mathbf{y}_i \mathbf{s}_i^T)$ and \mathcal{B}_k^0 is initialized as a simple positive-definite matrix. $\langle \cdot, \cdot \rangle$ denotes the Frobenius inner product. By using formula (20), we use a two-loop recursion to calculate the search direction η_k to reduce complexity because this method does not need to store \mathcal{B}_k . The two-loop recursion is presented in Algorithm 1.

To ensure the robustness and convergence of our R-L-BFGS algorithm in the non-convex problem, we incorporate a Cautious Update Check [18]. This strategy ensures that the new pair $(\mathbf{s}_k, \mathbf{y}_k)$ is admitted into the history only if it satisfies a more stringent, adaptive curvature condition: $\langle \mathbf{s}_k, \mathbf{y}_k \rangle_{\Theta_{g,k+1}} / \langle \mathbf{s}_k, \mathbf{s}_k \rangle_{\Theta_{g,k+1}} \geq \nu(\|\mathbf{g}_k\|)$, where $\nu(\cdot)$ is a

Algorithm 2 Proposed R-L-BFGS Optimization Algorithm

Input: Problem parameters $\mathbf{f}_k, \mathbf{G}_b, G, \rho, \tau, \mathbf{w}$.
Output: Optimal matrices Θ_t^*, Θ_r^* .

- 1: **for** $g = 1 : G$ **do**
- 2: **Initialization:** $k = 0, \mathcal{B}_0$, empty history buffers S, Y, P , iteration number k_{max} ; Compute $\eta_0 = -\mathbf{g}_0$.
- 3: **while** $k < k_{max}$ and $\|\mathbf{g}_k\| \geq \epsilon$ **do**
- 4: Find the step size α_k via Backtracking line search.
- 5: Compute the new iteration $\Theta_{g,k+1} = R_{\Theta_{g,k}}(\alpha_k \eta_k)$.
- 6: Compute \mathbf{g}_{k+1} using (18).
- 7: Transport all vectors in history buffers $\{S, Y\}$ from $T_{\Theta_{g,k}} \mathcal{M}$ to $T_{\Theta_{g,k+1}} \mathcal{M}^1$.
- 8: Compute new $\mathbf{s}_k, \mathbf{y}_k$ and add $(\mathbf{s}_k, \mathbf{y}_k, \rho_k)$ to buffers S, Y, P based on the Cautious Update Check.
- 9: Use Algorithm 1 to compute η_{k+1} .
- 10: $k = k + 1$.
- 11: **end while**
- 12: Obtain $\Theta_g^* = \Theta_{g,k}$ and extract $\Theta_{t,g}^*, \Theta_{r,g}^*$ using (21).
- 13: **end for**
- 14: **Return** $\Theta_{t/r}^*$.

Algorithm 3 Overall Beamforming Design Framework

Input: All channels $\mathbf{h}_{l,k,d}, \mathbf{f}_k, \mathbf{G}_l$ where $\forall l \in \mathcal{L}, k \in \mathcal{K}$.
Output: $\Theta_t^*, \Theta_r^*, \mathbf{w}^*$.

- 1: Initialize $\Theta_{t/r} = \text{diag}(\theta_{t/r,1}, \dots, \theta_{t/r,M}), \theta_{t/r,m} = \frac{1}{\sqrt{2}} e^{j\phi_{t/r,m}}, \phi_{t/r,m} \stackrel{\text{i.i.d.}}{\sim} \mathcal{U}[0, 2\pi), m = 1, \dots, M$; initialize \mathbf{w} using Zero-Forcing (ZF) method.
- 2: **while** no convergence of sum-SE **do**
- 3: Update τ by (6).
- 4: Update ρ by (6).
- 5: Update \mathbf{w} by solving (8).
- 6: Update Θ_t, Θ_r according to Algorithm 2.
- 7: **end while**
- 8: **Return** $\Theta_{t/r}^*, \mathbf{w}^*$, sum-SE.

strictly increasing function with $\nu(0) = 0$. The Cautious Update Check ensures a sufficient descent direction by maintaining a positive-definite Hessian approximation, which, in conjunction with the Armijo condition, guarantees convergence to a stationary point. At least we obtain reflective and transmissive matrices in each group from Θ_g^* , i.e.,

$$\Theta_{t,g}^* = [\Theta_g^*]_{1:\bar{M},:}, \quad \Theta_{r,g}^* = [\Theta_g^*]_{\bar{M}+1:2\bar{M},:}, \quad \forall g \in \mathcal{G}. \quad (21)$$

The procedure of obtaining $\Theta_{t/r}^*$ is outlined in Algorithm 2. Algorithm 3 outlines the overall beamforming design framework, with the complexity being $\mathcal{O}\{I(I_{RL}GM^3 + KLM^2 + I_a L^2 N^2 K^2)\}$. Here, I, I_{RL} , and I_a denote the iterations in Algorithm 3, Algorithm 2, and the PDS method for solving \mathbf{w} , respectively. The computational complexity is $\mathcal{O}\{I(I_{RL}M^3 + KLM^2 + I_a L^2 N^2 K^2)\}$ for the FC case ($G = 1$) and $\mathcal{O}\{I(I_{RL}M + KLM^2 + I_a L^2 N^2 K^2)\}$ for the SC case ($G = M$).

¹The vector transport we choose is isometric, ensuring that the inner product between history vectors remains unchanged during the transport process. Therefore, the scalar value stored in P remains unchanged during the iteration and does not need to be recalculated.

IV. SIMULATION RESULTS

This section presents the simulation results to show the performance of the BD-RIS-aided CF mMIMO system and our proposed algorithm. In our system model, the AP–BD-RIS, BD-RIS–UE, and AP–UE links are modeled by both large-scale and small-scale fading [3]. The large-scale fading is modeled by a distance-dependent path loss for a link i with distance d_i , given by $PL_i = \zeta_0(d_i/d_0)^{-\beta}$, where $\zeta_0 = -30$ dB at $d_0 = 1$ m and the path loss exponent $\beta = 2.2$ [10]. The small-scale fading is modeled by a Rician distribution with K-factor $K_{TR} = 5$ dB, incorporating both line-of-sight (LoS) and non-line-of-sight (NLoS) components. The LoS channel is represented as the outer product of transmit and receive array response vectors under a ULA assumption, while the NLoS component is modeled by a matrix of i.i.d. complex Gaussian variables [10]. The noise power at each user is set as $\sigma_k^2 = -80$ dBm, $\forall k \in \mathcal{K}$. And we assume that there are three APs placed at coordinates (0, 0), (0, 10), and (0, -10) meters, and the BD-RIS is placed at (200, 0) meters. The UEs are placed on the left and right halves of a circle centered at the BD-RIS, with two UEs in each half, and a radius of 2.5 meters. In our simulation, six curves are defined as follows: 1) GC/FC: group-connected/fully-connected BD-RIS; 2) STAR-RIS: single-connected BD-RIS; 3) RIS: traditional diagonal RIS; and 4) 1-bit/2-bit phase shift: non-ideal RIS phase shift case, denoting the cases \mathcal{F}_2 and \mathcal{F}_3 in [3].

Fig. 1a shows the sum-SE of the system under different architectures in relation to the number of iterations. We can observe that the proposed algorithm always converges in a limited number of iterations under different BD-RIS architectures, which also demonstrates the robustness of our proposed algorithm. The result also highlights that BD-RISs can achieve superior sum-SE performance compared to RISs. We present the sum-SE as a function of the transmit power per AP in Fig. 1b. First, regarding the BD-RIS architectures, the performance is consistently ranked as FC > GC > SC, which validates that higher degrees of freedom in the BD-RIS connectivity lead to superior performance. Second, for every architecture, the performance of the R-BFGS algorithm and our proposed R-L-BFGS algorithm are nearly identical and consistently outperform the Riemannian Conjugate-Gradient (R-CG) method. This demonstrates the benefit of leveraging approximate second-order curvature information to converge to higher-quality solutions. The fact that the limited-memory R-L-BFGS can match the performance of the computationally intensive R-BFGS highlights its efficacy for this problem. Fig. 1c illustrates the robustness of the proposed beamforming scheme to CSI error. We model the estimated channel \hat{h} as $\hat{h} = h + e$, where h is the real channel and e is the Gaussian estimation error with variance $\sigma_e^2 = \delta|h|^2$ and zero mean [3]. δ quantifies the CSI error level as the ratio of the error power σ_e^2 to the channel gain $|h|^2$. As can be observed in Fig. 1c the sum-SE of all architectures degrades as δ increases. Particularly, the system performance suffers a loss of 5% when $\delta = 0.1$ and a loss of 20% when $\delta = 0.3$. Therefore, the proposed algorithm shows strong robustness to CSI error. Fig. 1d provides a comprehensive analysis of the computational performance by comparing the per-iteration CPU time

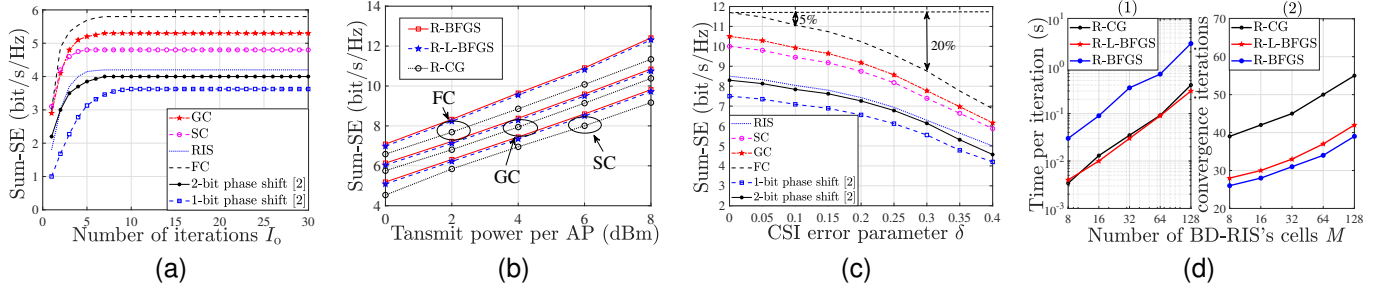


Fig. 1: (a): Sum-SE against the number of iterations I_0 with $L = 3, K = 4, M = 16, N = 2, P_{l,max} = 0.001, G = 2$. (b): Sum-SE against the transmit power per AP with $L = 3, K = 4, M = 32, N = 2, G = 2$. (c): Sum-SE against the CSI error parameter δ with $L = 3, K = 4, M = 32, N = 2, P_{l,max} = 0.003, G = 2$. (d): Computational complexity comparison: (1) average CPU time per iteration and (2) average number of iterations to convergence, versus the number of BD-RIS cells M . The experimental platform is built on a Windows 11 system with 13th Gen Intel(R) Core(TM) i7-13650HX.

(Fig. 1d (1)) and the required convergence iterations (Fig. 1d (2)) for the R-L-BFGS, R-CG, and R-BFGS algorithms. As shown in Fig. 1d (1), the per-iteration cost of R-BFGS grows at an unsustainable rate, confirming its impracticality for large-scale systems, while the costs of R-L-BFGS and R-CG are nearly identical. Fig. 1d (2) shows that our proposed R-L-BFGS algorithm requires significantly fewer iterations to converge than the first-order R-CG method, approaching the rapid convergence of the R-BFGS method. For instance, when the number of BD-RIS cells is $M = 32$, the R-L-BFGS algorithm converges in approximately 32 iterations, compared with about 45 iterations for R-CG, yielding a reduction of nearly 28% in iteration count. Meanwhile, its per-iteration CPU time (around 10^{-2} s) remains almost the same as R-CG and is markedly lower than that of R-BFGS (around 10^{-1} s). Therefore, our R-L-BFGS algorithm demonstrates an optimal trade-off: it leverages approximate second-order information to reduce the number of iterations, a benefit that far outweighs its minor per-iteration overhead, thus achieving superior overall computational efficiency compared to the R-CG baseline.

V. CONCLUSION

In this correspondence, we have investigated the sum-SE maximization problem in a hybrid BD-RIS-aided CF mMIMO system. We proposed a comprehensive beamforming design framework based on alternating optimization. To address the non-convex subproblem, we develop a robust and computationally efficient algorithm based on R-L-BFGS on the Stiefel manifold. Simulation results have shown that our algorithm can achieve faster convergence and find higher-quality solutions. Therefore, our proposed algorithm has great potential for practical application of hybrid BD-RIS in CF mMIMO systems. Future work of robust beamforming under imperfect CSI and the extension of our framework to novel BD-RISs, such as stem-connected and band-connected architectures, will provide greater theoretical and practical value.

REFERENCES

- [1] H. Viswanathan and P. E. Mogensen, "Communications in the 6G era," *IEEE Access*, vol. 8, pp. 57 063–57 074, 2020.
- [2] B. Xu, J. Zhang, Z. Chen, B. Cheng, Z. Liu, Y.-C. Wu, and B. Ai, "Channel estimation for Rydberg atomic receivers," *IEEE Wirel. Commun. Lett.*, Sep., 2025.
- [3] Z. Zhang and L. Dai, "A joint precoding framework for wideband reconfigurable intelligent surface-aided cell-free network," *IEEE Trans. Signal Process.*, vol. 69, pp. 4085–4101, Jun. 2021.
- [4] T. Van Chien, H. Q. Ngo, S. Chatzinotas, M. Di Renzo, and B. Ottersten, "Reconfigurable intelligent surface-assisted cell-free massive MIMO systems over spatially-correlated channels," *IEEE Trans. Wireless Commun.*, vol. 21, no. 7, pp. 5106–5128, Dec. 2022.
- [5] Z. Sui, H. Q. Ngo, T. V. Chien, M. Matthaiou, and L. Hanzo, "RIS-assisted cell-free massive MIMO relying on reflection pattern modulation," *IEEE Trans. Commun.*, vol. 73, no. 2, pp. 968–982, Aug. 2025.
- [6] J. Zheng, J. Zhang, H. Du, R. Zhang, D. Niyato, O. A. Dobre, and B. Ai, "Rate-splitting for cell-free massive MIMO: Performance analysis and generative AI approach," *IEEE Trans. Commun.*, vol. 73, no. 4, pp. 2431–2447, Apr. 2025.
- [7] Y. Zhu, J. Zhang, E. Shi, Z. Liu, C. Yuen, and B. Ai, "Joint power allocation and phase shift design for stacked intelligent metasurfaces-aided cell-free massive MIMO systems with MARL," 2025. [Online]. Available: <https://arxiv.org/abs/2502.19675>
- [8] Z. Ma, R. Zhang, B. Ai, Z. Lian, L. Zeng, D. Niyato, and Y. Peng, "Deep reinforcement learning for energy efficiency maximization in RSMA-IRS-assisted ISAC system," *IEEE Trans. Veh. Technol.*, pp. 1–6, 2025.
- [9] B. Xu, J. Zhang, H. Du, Z. Wang, Y. Liu, D. Niyato, B. Ai, and K. B. Letaief, "Resource allocation for near-field communications: Fundamentals, tools, and outlooks," *IEEE Wireless Commun.*, vol. 31, no. 5, pp. 42–50, Jul. 2024.
- [10] H. Li, S. Shen, and B. Clerckx, "Beyond diagonal reconfigurable intelligent surfaces: From transmitting and reflecting modes to single-, group-, and fully-connected architectures," *IEEE Trans. Wireless Commun.*, vol. 22, no. 4, pp. 2311–2324, Apr. 2023.
- [11] Z. Wu and B. Clerckx, "Beyond-diagonal RIS in multiuser MIMO: Graph theoretic modeling and optimal architectures with low complexity," *IEEE Trans. Inf. Theory*, to appear, 2025.
- [12] X. Zhou, T. Fang, and Y. Mao, "A novel Q-stem connected architecture for beyond-diagonal reconfigurable intelligent surfaces," in *Proc. 2025 IEEE Int. Conf. Commun. (ICC)*, Jun. 2025, pp. 6880–6885.
- [13] Z. Sui, H. Q. Ngo, M. Matthaiou, and L. Hanzo, "Performance analysis and optimization of STAR-RIS-aided cell-free massive MIMO systems relying on imperfect hardware," *IEEE Trans. Wireless Commun.*, vol. 24, no. 4, pp. 2925–2939, Jan. 2025.
- [14] T. D. Hua, M. Mohammadi, H. Q. Ngo, and M. Matthaiou, "Cell-free massive MIMO SWIPT with beyond diagonal reconfigurable intelligent surfaces," *IEEE Trans. Commun.*, to appear, 2025.
- [15] X. Zhou, T. Fang, and Y. Mao, "Joint active and passive beamforming optimization for beyond diagonal RIS-aided multi-user communications," *IEEE Commun. Lett.*, pp. 1–1, Jan. 2025.
- [16] K. Shen and W. Yu, "Fractional programming for communication systems—part I: Power control and beamforming," *IEEE Trans. Signal Process.*, vol. 66, no. 10, pp. 2616–2630, Mar. 2018.
- [17] P.-A. Absil, R. Mahony, and R. Sepulchre, *Optimization Algorithms on Matrix Manifolds*. Princeton University Press, 2009.
- [18] W. Huang, P.-A. Absil, and K. A. Gallivan, "A Riemannian BFGS method for nonconvex optimization problems," in *Proc. ENUMATH. Cham, Switzerland: Springer*, 2016, pp. 627–634.